

Probing Protein Ensemble Rigidity and Hydrogen-Deuterium exchange

Adnan Sljoka^{1‡} and Derek Wilson^{2§}

¹Department of Mathematics and Statistics, York University,
4700 Keele Street, Toronto, M3J 1P3, Canada

² Chemistry Department, York University,
4700 Keele Street, Toronto, M3J 1P3, Canada

Abstract.

Protein rigidity and flexibility can be analyzed accurately and efficiently using the program FIRST. Previous studies using FIRST were designed to analyze the rigidity and flexibility of proteins using a single static (snapshot) structure. It is however well known that proteins can undergo spontaneous sub-molecular unfolding and refolding, or conformational dynamics, even under conditions that strongly favour a well-defined native structure. These (local) unfolding events result in a large number of conformers that differ from each other very slightly. In this context, proteins are better represented as a thermodynamic ensemble of ‘native-like’ structures, and not just as a single static low-energy structure.

Working with this notion, we introduce a novel FIRST-based approach for predicting rigidity/flexibility of the protein ensemble by (i) averaging the hydrogen bonding strengths from the entire ensemble and (ii) by refining the mathematical model of hydrogen bonds. Furthermore, we combine our FIRST-ensemble rigidity predictions with the ensemble solvent accessibility data of the backbone amides and propose a novel computational method which uses both rigidity and solvent accessibility for predicting hydrogen-deuterium exchange (HDX). To validate our predictions, we report a novel site specific HDX experiment which characterizes the native structural ensemble of Acylphosphatase from hyperthermophile *Sulfolobus solfataricus* (Sso AcP).

The sub-structural conformational dynamics that is observed by HDX data, is closely matched with the FIRST-ensemble rigidity predictions, which could not be attained using the traditional single ‘snapshot’ rigidity analysis. Moreover, the computational predictions of regions that are protected from HDX and those that undergo exchange are in very good agreement with the experimental HDX profile of Sso AcP.

Key Words: protein flexibility, FIRST, Hydrogen/Deuterium exchange, pebble game algorithm, solvent accessibility, NMR ensembles.

PACS numbers: 82.56.Pp, 87.14.E-, 87.15.A-, 87.15.H-, 87.15.hp, 87.15.-v, 87.64.kj

‡ Supported in part under a grant from NSERC (Canada). Email: adnanslj@matstat.yorku.ca

§ Supported by NSERC (Canada) Discovery Grant # 341925. Email: dkwilson@yorku.ca

1. Introduction

It has long been accepted that protein structural flexibility and dynamics is as critical for protein function as its 3D-structure [1, 9]. Accurate measurements of flexibility and dynamics of proteins can help us interpret the relationship between structure and function, and has significant biological implications in medicine and drug design [22, 34, 21, 67]. Being able to give fast predictions of flexible and rigid regions in the proteins and its dynamics is an important area of research in computational biology, particularly in high throughput studies.

Determining flexible and rigid regions in a protein and understanding its motions is a complex task. The main difficulty is that conformational fluctuations are rapid, transient and result in structures that are spectroscopically indistinguishable from the ground-state. A wide range of experimental data (NMR techniques such as order parameter measurements, relaxation dispersion, hydrogen/deuterium exchange data, etc.) can provide some limited insights [19, 27, 46]. Computational methods have also facilitated enormous strides in this area [6, 33, 34, 43, 54]. Molecular dynamics (MD) simulations is traditionally used to probe protein mobility and flexibility, but its main downside is that it takes a prohibitive amount of computational power to investigate the functionally relevant micro- and millisecond time-scales.

Given the rapid growth in the number of entries in the protein data bank and the size of the solved protein structures, combined with the severe limitation of computational power and resources needed to study protein flexibility and dynamics with traditional methods, there is a tremendous need to develop faster computational methods. One such computationally fast new method is FIRST [16, 34] (Floppy Inclusion and Rigid Substructure Topography) or its earlier version PROFLEX [35] along with its extensions, such as FRODA [60].

FIRST (see Section 2.1) is based on a well established mathematical theory of Rigidity Theory [62, 63] and concepts in solid state physics [57]. Computationally, FIRST uses the combinatorial pebble game algorithm [37, 56, 63], which performs the constraint counting in the molecular multigraph (constraint network) in order to match the degrees of freedom with various biochemical constraints, and outputs all the rigid and flexible regions in the protein. While considerable computational power is needed to study protein flexibility with MD simulations, FIRST can predict the rigid clusters and flexible connections (known as the *rigid cluster decomposition*) in a matter of seconds. Numerous studies have thoroughly demonstrated that FIRST gives accurate predictions of flexibility and rigidity in proteins [21, 23, 24, 34] and RNA [18].

1.1. Extending FIRST to Protein ensembles

In the ‘new view’ of protein folding and energy landscapes, the native state is represented as the minimum in a narrow, symmetric free energy well [11]. Even under native conditions, proteins occupying this well can undergo local conformational fluctuations

that occur on a wide range of time-scales, from microseconds to hours, sampling a distribution of native like conformational substates, referred to as the ‘native-state ensemble’ [2, 9, 17, 27, 22, 41, 47, 51]. The native-state ensemble is important to aspects of protein function including stability, cooperativity and catalysis [13, 30, 36, 41, 64]. There is therefore a strong incentive to characterize the native structural ensemble with a view to isolating those conformers that are most associated with biological activity.

One major source of experimental data that can provide structural insight on the native state conformational ensemble is available in the protein data bank (PDB) [5]. NMR structures in the PDB are consistently expressed as ‘ensembles’ of structures, where the entire ensemble represents a possible solution set to the NMR structure determination problem [59]. Some promising work in the area of ensemble refinement suggests that structures solved by x-ray crystallography, where discrete conformations of the atomic coordinates can be identified, would be better represented as a set of multiple conformers [32, 38]. Unfortunately, to date, only a small number of X-ray crystal structures with several conformers are available in the PDB [38].

One clear limitation of the current FIRST method (and equivalent implementations) is that it is primarily designed to perform the flexibility analysis using a single structure (snapshot) of a protein. When the protein structure is represented with a collection of conformers, particularly the NMR solved structures, previous FIRST studies would perform the rigidity/flexibility analysis only on a selected single structure (i.e. typically using the ‘most-representative’ structure-model defined by the authors of the NMR structure), completely neglecting the information encoded in the other structures of the ensemble. In fact, there has been no distinction in the FIRST analysis of X-ray structures with single snapshots and those from NMR solved structures.

By selecting only a single NMR structure, not only is the crucial ensemble information omitted, but the development of the constraint network purely from the single structure can make the rigidity/flexibility analysis more sensitive to the quality of the structure (snapshot) selected [34]. It is well known that vary small structural variations in the constraint network (i.e. breaking of a few hydrogen bonds and in some extreme cases a single hydrogen bond) can have a significant effect on the rigid cluster decomposition, breaking a single rigid cluster into numerous smaller rigid regions [49, 61]. It is then natural to hypothesize that analyzing multiple snapshots should alleviate these sensitivities and deficiencies of the FIRST analysis, in particular the dependence of rigidity predictions on the selection of modelled non-covalent interactions, especially hydrogen bonds. Clearly, better ways of predicting rigidity of conformational ensemble than the current FIRST model are desirable.

A major objective of this paper is to enhance the predictive power of FIRST for dynamics by conducting the analysis on the ensemble. We will achieve ensemble-based prediction from FIRST by averaging the hydrogen bonding interactions over all the individuals structures (i.e. NMR models) of the ensemble, and by a refinement of the mathematical model of hydrogen bonds, to give a single ensemble FIRST prediction (see

Materials and Methods section). We will illustrate that the FIRST-ensemble predictions can overcome some of the limitations of the traditional single (static) snapshot analysis, and should provide us with a more sensible and improved picture of rigidity/flexibility.

To test our method we will apply it to the native structural NMR ensemble of Acylphosphatase from hyperthermophile *Sulfolobus solfataricus* (Sso AcP) (figure 1). Sso AcP is a 101-residue protein, which belongs to the acylphosphatase-like structural family [4]. The hyperthermophile nature of Sso AcP also offers a unique opportunity to apply the FIRST analysis to an enzyme that is expected to be non-functional at room temperature due to rigidity. We will compare the traditional FIRST single snapshot rigidity prediction with our modified FIRST prediction over the entire ensemble. The validity of these predictions is then tested by comparison with an experimentally derived picture of the ensemble acquired via NMR-based hydrogen/deuterium exchange (HDX) measurements. Our FIRST-ensemble approach is quite general and can equally be applied to an ensemble of snapshots generated by other techniques, for instance conformers extracted from coarse-grain MD simulations [21, 42].

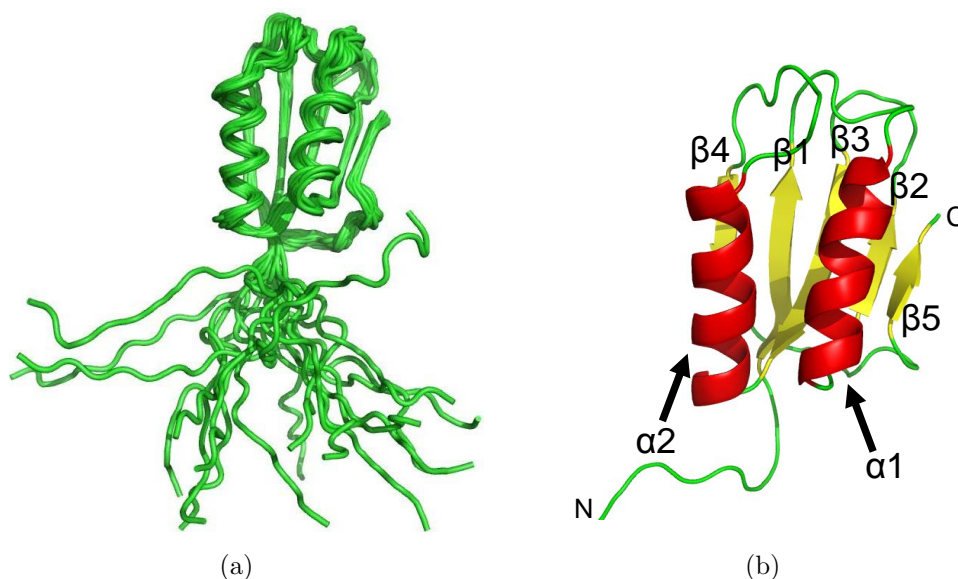


Figure 1. NMR derived 3-dimensional structure of Acylphosphatase from hyperthermophile *Sulfolobus solfataricus* (Sso AcP) (pdb id: 1y9o). (a) The entire structural ensemble (20 models) is shown in ribbon representation (images generated with Pymol [48]) (b) the first model (i.e. most representative structure) is shown in the cartoon representation and coloured and labeled according to its secondary structure.

1.2. Combined Rigidity and Solvent Accessibility Analysis is a Computationally Facile Predictor of Hydrogen/Deuterium Exchange

HDX is a powerful experimental technique as it can provide us with direct information about protein's dynamics and structural stability [2, 15]. It is particularly useful as it is sensitive to the entire structural ensemble, even to the most rarely sampled high energy

conformers. At physiological pH, HDX is a process in which amide protons on the polypeptide ‘backbone’ and ‘exchangeable’ protons on some side chains undergo base-catalyzed exchange with solvent [14]. Experimental measurements of HDX are typically confined to the backbone amide protons, which are involved in hydrogen bonding for the maintenance of secondary structure. Since the hydrogen bond must first ‘break’ in order for exchange to occur, HDX can be used to provide a semi-quantitative measurement of local thermodynamic stability in secondary structures. HDX can also occur when the amide hydrogens become exposed (accessible) to the solvent [15]. Thus, the observed rate of backbone amide exchange is a function of hydrogen bond strength and solvent accessibility [14, 65].

Using NMR techniques it is possible to monitor backbone amide proton signals as a function of time after exposure to deuterated water (D_2O) (deuterium does not produce a signal in conventional Heteronuclear Single Quantumn Coherence (HSQC) experiments), and assign ensemble exchange rates to individual residues (backbone amide protons). In our study, an experimental residue-specific HDX-profile was obtained for Sso Acp, and residues were classified into a range of categories, from very slow exchangers to very fast exchangers. Residues that do not exchange and residues that are very slow exchangers are either buried away from the solvent or they are found in very stable and rigid regions of a protein with strong hydrogen bonding interactions.

Although experimental methods for measuring HDX are well established (using NMR and Mass Spectrometry technologies), they can be very costly and time demanding. Only a few computational methods have been suggested [12, 40]. Devising new fast algorithms that can give rapid predictions of the regions in the protein that are protected from HDX and regions that are not protected would be very valuable. For instance, predictions of HDX (together with sequence homology) is used to predict 3-dimensional structures of unknown proteins [40]. By avoiding the bottlenecks associated with the slow experimental techniques, fast computational HDX prediction algorithms can also enable high throughput analysis.

As HDX depends on both structural stability and solvent accessibility, we hypothesize that combining rigidity predictions with solvent accessibility data should provide us direct insight into regions that are most likely protected from HDX and regions that are not protected from HDX. More specifically, if a region of a protein is rigid (particular over the ensemble) it will have a sufficient number of constraints (a rich hydrogen bonding network) to prevent it from undergoing HDX. Similarly, regions whose backbone amides (NH) are buried (inaccessible) from the solvent, should not be good exchangers. On the other hand, backbone amides in flexible and solvent accessible regions should be among the fast exchangers.

In order to test this hypothesis, and as the main goal of the paper, we will introduce a new computational method for predicting HDX, which combines our FIRST-ensemble rigidity predictions with computationally generated ensemble solvent accessibility data (see materials and methods) of the backbone amide (NH).

In summary, the following two new contributions are based on this work:

- development of an ensemble-based FIRST method for predicting protein flexibility/rigidity
- an introduction of a novel computational method which combines FIRST-ensemble rigidity predictions and ensemble solvent accessibility data as a predictor of HDX (an ensemble measurement);

We will apply these techniques on the case study protein Sso AcP, and the predictions will be compared with our experimentally obtained HDX data. To our best knowledge, this is first analysis which uses both rigidity and solvent accessibility for predicting HDX.

2. Materials and Methods

2.1. FIRST

Starting with the 3-dimensional snapshot of a protein structure (PDB file), FIRST generates a constraint multigraph (a graph which allows multiple edges between vertices) [25, 63], where the molecule is viewed as a body-hinge engineered structure of fixed units (atoms or bodies with their bond angles as rigid units, bonds as potential hinges) plus other molecular constraints extracted from the local geometry. In the constraint multigraph, vertices represent atoms and edges represent the distance constraints corresponding to covalent bonds, hydrogen bonds and hydrophobic interactions.

The strength of each potential hydrogen bond is calculated based on its local donor atom–hydrogen–acceptor atom (angular and distance) geometry (see [23, 34, 61] for details). Hydrophobic contacts or tethers are modelled as any close contacts between pairs of carbon and/or sulfur atoms [34]. Once all the constraints are considered and the user has selected a hydrogen bond energy cutoff value, the pebble game algorithm rapidly decomposes a multigraph (protein) into rigid clusters and flexible regions [23, 34, 61]. In every rigid cluster, all bonds will be non-rotatable and all its atoms can only move as a single rigid body. On the other hand, flexible regions lack sufficient number of constraints to further restrict their internal motions. A protein will normally be composed of several large rigid clusters, which are connected by flexible regions. For further details consult the FIRST user manual and references [21, 61, 23, 25, 34, 24].

2.2. Comments on Hydrogen Bonds

The output of FIRST is almost entirely dependant on the set of modelled hydrogen bond constraints. Revisiting important features of hydrogen bonds and understanding the limitations of the current hydrogen bond mathematical rigidity model will help us consider refinements and facilitate a meaningful extension of FIRST predictions to structural ensembles.

The hydrogen bond energy cutoff will distinguish between weak and strong hydrogen bonds. However, no further quantitative distinction is made; any two hydrogen bonds that meet the threshold are included as constraints and remove the same number of degrees of freedom [34, 61]. In fact, in terms of the mathematical model of rigidity, the hydrogen bonds that pass the cutoff are modelled equivalently to the covalent bonds; for each hydrogen bond, five bars (edges) are placed between the hydrogen and the acceptor atom.

There are further uncertainties which are unique to hydrogen bonds that need to be considered. Molecular dynamics simulations have confirmed that many hydrogen bonds have short life times and undergo ‘flickering’ on the order of tens of picoseconds to a few nanoseconds [42, 55]. This is particularly true in the flexible and dynamic regions of the protein, where hydrogen bonds spontaneously break and reform to adjust to the conformational changes of atoms. Every conformation that the protein samples under native conditions has a particular set of hydrogen bonds, which can be significantly different in another conformation due to the local changes in hydrogen bonding geometry. The authors of [61] report that small variations in the donor-acceptor distance can lead to substantial changes in the hydrogen bond energy strengths. Consequently, FIRST runs on the snapshots generated with molecular dynamics simulation [42] have significant differences in the rigid cluster decompositions. To address the ‘flickering’ (time-dependant) nature of hydrogen bonds and the fluctuations in hydrogen bond strengths (i.e. geometry), Mamonova et al. [42] have incorporated the lifetimes of hydrogen bonds (how often is each hydrogen bond present over the MD simulation) into FIRST analysis. This approach gave an improved FIRST prediction which better matched the experimental evidence and molecular dynamics simulations.

Whenever we are given a collection of snapshots (i.e. NMR ensemble), in order to obtain more accurate and realistic FIRST predictions on the ensemble it will be crucial to consider a refinement of the current hydrogen bond model. A natural first step in this refinement is to obtain the average hydrogen bond strength for each hydrogen bond over all NMR conformers. Only hydrogen bonds that have strong average strengths (energy) over the entire ensemble will be included in the constraint multigraph (see Algorithm 2.1 for details). Furthermore, we will also modify the rigidity model of hydrogen bonds by considering the persistence of hydrogen bonds. Instead of always using 5 bars between the acceptor and donor atoms, we will allow the number of bars (edges) to vary between 1 and 5 (see figures 2 and 3). By varying the number of bars, we can adjust the number of DOF that the hydrogen bond should remove based on its persistence over the ensemble. If the hydrogen bond does not persist over all snapshots, it will be subject to a penalty. In other words, if the average energy strength of a particular hydrogen bond is sufficiently high over the entire ensemble, yet it is not present (or very weak) in several snapshots, the hydrogen bond will still be included as a constraint. However, given that there will be a bar(s) penalty for this kind of hydrogen bond, a constraint with say 2 or 3 bars will remove less DOF from the overall system than the traditional

5 bar constraint. This permits us to gradually weaken those bonds that may not persist in all the snapshots (models).

This type of revised modelling of hydrogen bonds via averaging the strengths over an ensemble and varying the number of bars should give us a more tuned and refined representation of hydrogen bonds. It also facilitates the move away from the simple ‘on/off’ type of modelling of hydrogen bonding constraints that has been applied in previous FIRST studies.

2.3. First-ensemble procedure

We now describe the procedure that gives a single FIRST prediction (rigid cluster decomposition) on the entire ensemble from an NMR protein structure. We call such predictions *FIRST-ensemble*. Typical NMR file will contain 20 models that best fit the NMR data, so we take $m = 20$ below.

All the rigidity/flexibility runs on an NMR solved structure of Sso AcP (pdb id: 1y9o) are performed using a standard FIRST software implementation. In all the FIRST predictions on both the individual NMR snapshots and on the FIRST-ensemble predictions, we have set the hydrogen bond energy cutoff to -1.0 kcal/mol, that is we include only those hydrogen bonds whose energy is less than (more favourable than) -1.0 kcal/mol.

Algorithm 2.1 – *FIRST-ensemble procedure*:

Input: NMR PDB file (or other source of protein ensembles).

Output: single FIRST rigidity/flexibility ensemble prediction (i.e. rigid cluster decomposition).

(1.) Run FIRST on every NMR model m ($m = 1..20$) using a hydrogen bond energy cutoff of 0 kcal/mol and obtain the energy strength E_i^m for every hydrogen bond i .

(2.) Calculate the average energy strength E_{AVGi} for each hydrogen bond i over all 20 models:

$$E_{AVGi} = \frac{\sum_{m=0}^{20} E_i^m}{20}$$

(3.) Use the following criteria to assign the bar (edge) penalty between hydrogen and acceptor atoms for each hydrogen bond i :

(a) Define hydrogen bond i as being present in a specific model (snapshot) if its energy strength is less than (more favourable than) -0.5 kcal/mol. Denote the total number of times hydrogen bond i is present out of 20 models as N_i .

(b) Assign the number of bars (edges) B_i (correction factor) for every hydrogen bond i , using the following rule: $B_i = \lceil \frac{N_i}{20} \times 5 \rceil$ (where $\lceil x \rceil$ is a ceiling function, see figure 3)

(4.) Select the first NMR model (any model could be selected - see supplementary information and discussion below) and run FIRST

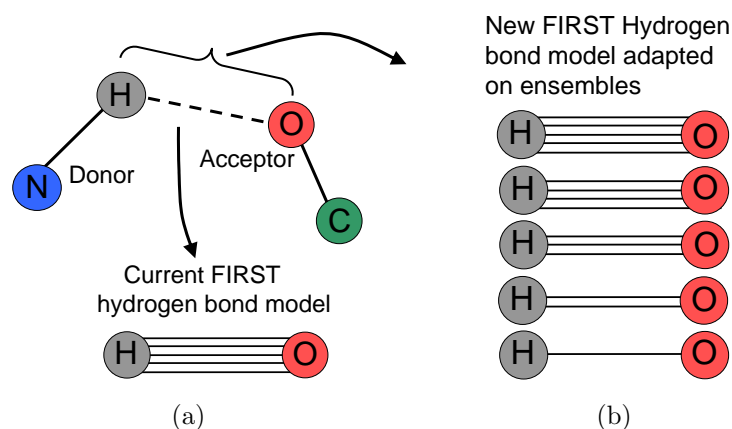


Figure 2. In FIRST hydrogen bonds are modelled with 5 bars (edges, constraints) between hydrogen and acceptor atoms (a). In the FIRST-ensemble predictions we allow the number of bars to vary between 1 and 5, depending on the persistence of a hydrogen bond over all structures in the ensemble (b).

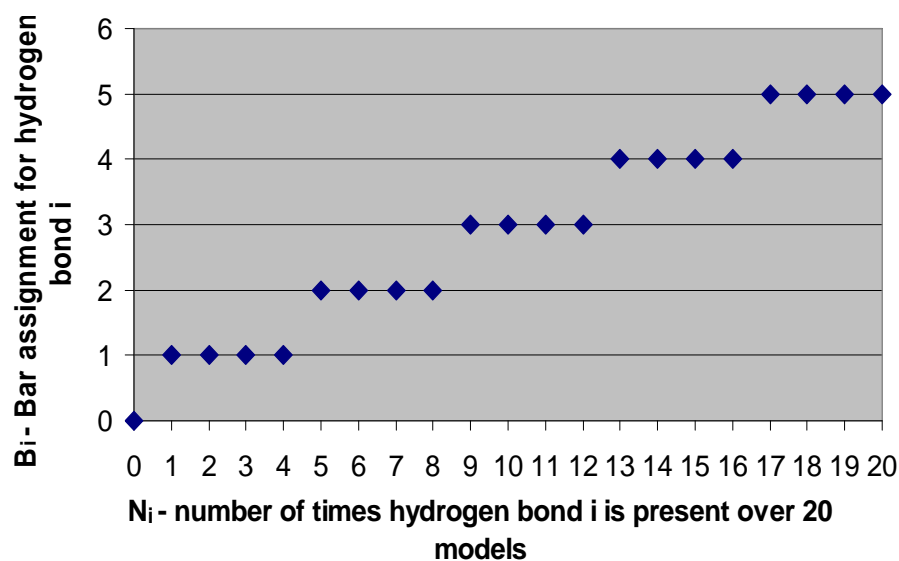


Figure 3. The number of bars (edges) B_i that are assigned for hydrogen bond i depends on how often the bond is present in the ensemble.

In step 1. we run FIRST with energy cutoff of 0 kcal/mol as this cutoff would consider all weak and strong hydrogen bonds. In the FIRST-ensemble approach, we still use an energy cutoff to distinguish weak from strong hydrogen bonds (averaged over the ensemble), with the added feature that the correction factor B_i allows us to incorporate the measure of the persistence of a hydrogen bond over the ensemble. Consider for instance a hydrogen bond i that is present in 10 out of 20 models, with relatively strong individual energies E_i^m over the 10 models. The average E_{AVG_i} strength may still be relatively (negatively) high, such that it passes the energy cutoff (in our study -1.0

kcal/mol). In this case this bond would be included as a constraint in the rigidity analysis. The usefulness of correction factor B_i can be seen as it takes into account the absence (weak energy, bad geometry) of this hydrogen bond in the remaining 10 models, giving it a 2 bar penalty, and an assignment of 3 bars (see figures 2 and 3).

2.4. Solvent Accessibility Calculations

The solvent ‘accessible surface area’ (ASA) is the measure to which atoms on the protein surface are able to make contact with water. ASA is defined as the surface area traced out by the center of a water sphere (radius of about 1.4 angstroms) as it is rolled over the surface of the protein [7, 58]. It is a standard practice to convert the ASA to its normalized form – ‘relative solvent accessibility’ (RSA), which is the ratio of ASA in the current folded conformation to the ASA in the extended-unfolded conformation taken in the Gly-X-Gly tripeptide state [50, 58]. Given that the experimental HDX on Sso AcP measures exclusively the HDX rates of backbone amide protons, we are only interested in obtaining solvent accessibility of the backbone amides (NH). We will use the WHATIF [58] procedure to determine the RSA for all backbone nitrogens of Sso AcP in all the 20 models of an NMR ensemble. We then calculate the average (over the 20 NMR models) RSA for every backbone nitrogen.

We are primarily interested in finding the set of residues whose (ensemble averaged) backbone amides (NH) are completely or almost completely buried from the solvent, as these residues should not be undergoing exchange. The reported RSA cutoffs to distinguish buried states in the literature have varied greatly, with values in the 0% to 15% range [26, 39, 44, 50]. We define any residue as *almost completely buried* (or *solvent inaccessible*) if its backbone nitrogen RSA value (averaged over an entire ensemble) is less than 4 %, otherwise it is *exposed* (or *solvent accessible*). This strong cutoff allows us to select those residues whose backbone amide (NH) are closest to being completely buried. A smaller accessibility cutoff was not chosen due to potential numerical rounding approximations, and to eliminate the situations where a slight increase in average accessibility is a result of higher accessibility in one or two models.

When visualizing accessibility on a protein’s 3D structure, almost completely buried residues will be coloured blue. We further classify the exposed residues in the following categories (whose thresholds are somewhat arbitrarily selected but close to [50] for example): if the backbone nitrogen has accessibility which is between 4 % and 10 % we say that the corresponding residue is *somewhat exposed* (yellow), between 11 and 30 % *mostly exposed* (orange), and greater than 30 % *almost completely exposed* (red) (see figure 10). The results on Sso AcP are not sensitive to these threshold cutoffs and these remaining categories are solely assigned for easier visualization and comparison.

2.5. Combining FIRST-ensemble and Ensemble Solvent Accessibility as a Predictor of HD-exchange

Both rigidity/flexibility and solvent accessibility hold valuable information that can assist in predicting HDX. However, rigidity/flexibility or accessibility on its own provides only limited information. Consider a scenario where a given region of interest in the protein is flexible but its amide protons are completely buried away from the solvent, which would make this region a slow HD exchanger. If we did not have the solvent accessibility data, sole rigidity/flexibility predictions would not tell us about the lack of HDX in this region. In contrast, consider a rigid region which is accessible to the solvent. Using only solvent accessibility in this case is insufficient to probe HDX, since in a typical rigid region of a protein there is a significant number of strong hydrogen bonding interactions that will not transiently ‘break’ to allow HDX.

To probe our initial hypothesis, we now outline a procedure that combines the FIRST-ensemble rigidity predictions and solvent accessibility ensemble data, as a measure of HDX (an ensemble measurement).

Algorithm 2.2 – Rigidity and Accessibility as a prediction of HDX

Input: NMR PDB file (or other source of protein ensembles).

Output: Prediction of regions which are most likely protected from HDX (no exchange or slow exchangers), and regions which are likely to undergo exchange.

- (1.) Run the FIRST-ensemble procedure (Algorithm 2.1) to obtain the rigid cluster decomposition for the ensemble.
- (2.) Consider rigid clusters from (1.) and combine into a single coloured rigidity-region. Display this combined rigidity-region with a unique colour on the protein’s 3-dimensional structure, and choose a different colour for the remaining flexible regions. (We will colour the combined rigidity-region with the same colour as the largest rigid cluster, which is blue by default, and intervening flexible regions with gray.)
- (3.) Superimpose the average solvent accessibility regions (preferably using the colouring convention given in Section 2.4) on the remaining flexible regions (excluding α -helices and prolines) of the protein from step 2. ‘Almost-completely buried’ (inaccessible) regions should be displayed with the same colour as the combined-rigidity region (blue) in step (2.)

The combined rigidity-region and almost-completely buried (inaccessible) region (both coloured with blue) correspond to the regions that we predict will most likely be protected from HDX (i.e. slowest exchangers). The remaining regions: flexible (gray), somewhat exposed (yellow), mostly exposed (orange), and almost completely exposed (red) are the regions most likely not protected from undergoing HDX (i.e. fastest exchangers).

Due to the amphipathic character of α -helices, solvent accessibility is excluded for α -helices [39]. Solvent accessibility is not used for prolines as HDX is not assigned to prolines; amino acid proline has no backbone amide hydrogen.

2.6. Native State Hydrogen-Deuterium Exchange Experiment on Sso AcP

Materials and Protein Preparation and Purification. Mono- and di-basic sodium phosphate was purchased from Sigma (St. Louis, MO). Ultrapure water was generated in-house on a Millipore Advantage system. Uniformly ^{15}N labeled protein was produced from BL21(DE3) E. coli transformed using a pGEX-2T plasmid as described previously [8]. Briefly, transformed cells were grown for 8hrs at 38°C in M9 media with $^{15}\text{NH}_4\text{Cl}_2$ (Cambridge Isotope Laboratories, Andover, MA) as the sole Nitrogen source. Overexpression of Sso AcP was induced by IPTG when cultures reached $\text{OD} \sim 0.6$ (typically around 5 hrs). Cell lysis was by sonication. Sso AcP-GST was purified from the supernatant on a glutathione column with cleavage of the fusion protein by overnight digestion with Thrombin.

NMR Spectroscopy. ^1H - ^{15}N HSQC and FSHQC experiments were carried out on a cryoprobe Bruker Avance 500 Spectrometer at $T = 300\text{ K}$. Sample conditions were $150\mu\text{M}$ Sso AcP in 15 mM phosphate buffer (pH 7.0, 7.3 and 7.6). The low buffer concentration was to avoid sensitivity reduction in the cryoprobe. Water suppression was by excitation sculpting [28] or 3-9-19 watergate. Quadrature detection was by TPPI [3]. Spectral widths were 7200 Hz in t_2 dimension and 2000 Hz in t_1 . All spectra were composed of $t_2 = 1024 \times t_1 = 128$ complex points. Data was processed using the NMRPipe [10] and analyzed using Sparky [20].

CLEANEX-PM experiments. Proton/proton exchange measurements used the (CLEANEX-PM)-FHSQC pulse program introduced by Mori et al. in 1998 [29]. CLEANEX mixing times were between 10 and 50 ms. Assignment of peaks visible in (CLEANEX-PM)-FHSQC spectra was by comparison with an assigned reference FHSQC. CLEANEX experiments at pHs between 7.0 and 7.6 gave identical results. CLEANEX data were analyzed to give quantitative exchange rates using the ‘initial slope’ method described by Hwang et al in 1998 [29].

FSHQC HDX experiments. HDX measurements used FSHQC pulse sequence introduced by Mori et al. in 1995 [45]. In all experiments, the instrument was pre-shimmed using a blank sample (15 mM phosphate buffer in D_2O , pD 7.0, 7.3 and 7.6) in the NMR tube to be used in the HDX experiment. Sso AcP in 15 mM phosphate buffer (pH 7.0, 7.3 and 7.6) was concentrated to $\sim 1.5\text{ mM}$ using Vivaspin centrifugal concentrators (MWCO 5,000) and quickly added to the ‘pre-shimmed’, D_2O solution-containing NMR tube and mixed by inversion. The interval between mixing and the start of FHSQC acquisition was typically around 1.5 min. This includes time for introduction of the sample into the probe and brief manual re-shimming. Full FHSQCs were collected every 7.5 min for the first 3 hours. After three hours, the acquisition times were

lengthened by increasing n_s (the number of scans/ t_1). To acquire quantitative observed HDX rates k_{obs} , time-dependent FHSQC peak intensities I were normalized using n_s and fit to single exponential decay functions with offsets:

$$I = ae^{-k_{obs}t} + b \quad (1)$$

The extracted k_{obs} are related to conformational flexibility through primary sequence-specific extrinsic exchange rates k_{int} , which were predicted using the Sphere software [66]. When HDX occurs within the EX2 limit, the ratio k_{int}/k_{obs} (the ‘protection factor’) is directly related to conformational flexibility, expressed as an equilibrium between an ‘open’ (HDX-competant) and ‘closed’ (HDX-incompetant) state for each backbone amide.

3. Results and Discussion

3.1. Experimental HDX profile of Sso AcP

In figure 4 the experimental HDX profile of Sso AcP is overlaid on the 3-dimensional structure. We attained a high coverage native (ensemble) state HDX profile (87 % of residues were covered) on this hyperthermophile protein at moderate temperatures. Red and orange residues represent the very fast and fast exchangers, respectively. These appear exclusively in the loops and in the unstructured N-terminus tail region (first 12 residues), with the exception of one residue in the N-terminal end of α -helix 2 and one in the centre of α -helix 1 (see figure 1 for the labeling of secondary structures). Yellow residues represent the medium exchangers and blue the slowest exchangers (i.e. exchange not observed over three weeks after exposure to D_2O). Residues colored green were detected in the FHSQC, but at insufficient signal-to-noise to provide reliable exchange data. Details of these results are provided in the supplementary information.

In the gray regions no HDX measurements could be made as no NMR signal was detected (or the residue is a proline); most of these residues are found in unstructured parts of the protein. The notable exception is the cluster of residues bounded by Gln25 and Lys31, which are mostly found in the N-terminal end of α -helix 1. Of these only Val27 could be assigned in spite of the fact that these peaks were well dispersed in the reference spectrum. This suggests that the N-terminal half of α -helix 1 is unstructured and flexible, and likely undergoes large-amplitude ‘molten globule-like’ conformational dynamics. Residues undergoing molten-globule-like conformational dynamics are frequently not detectable by NMR due to extreme broadening of the HSQC signals.

Regions of the protein with high exchange rates (red and orange) correspond to the least protected regions, and regions with slowest exchange rates (blue) are the most protected. Majority of the slowest exchangers are found in the C-terminal half of α -helix 1, α -helix 2, and three central β -strands (strands 1, 2 and 3). α -helix 2 has significantly more slow exchangers than α -helix 1. The two halves of α -helix 1 are drastically different.

Unlike the N-terminal half which is very unstructured, the C-terminal half has only slow exchangers and is very well protected from undergoing exchange.

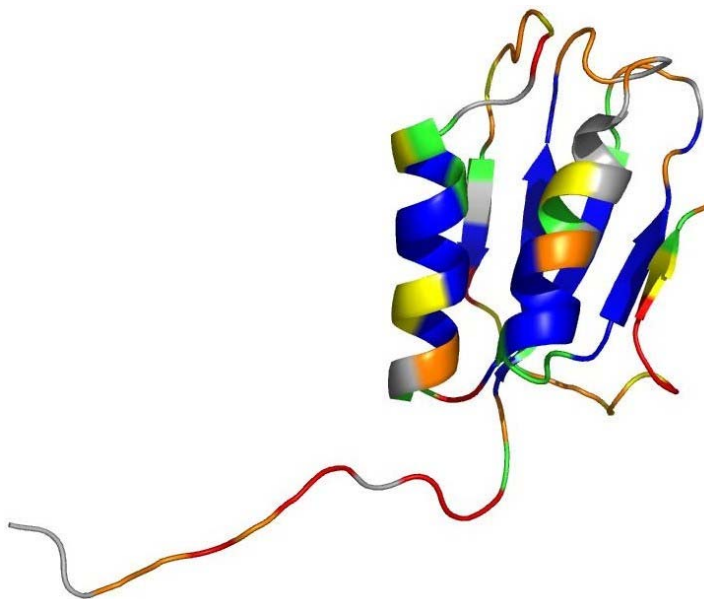


Figure 4. Hydrogen-Deuterium Exchange (HDX) profile of Sso AcP mapped on to the native structure (see text and supplementary information for details).

3.2. FIRST results on individual NMR models

Before acquiring our FIRST-ensemble predictions on Sso AcP, we first obtained the regular ‘single snapshot’ FIRST analysis on all 20 snapshots (models). The rigid cluster decomposition of the first ten models is displayed in figure 5.

There are only two large rigid clusters, corresponding to the blue and green regions in the two α -helices; flexible regions are coloured in gray. The β -sheet is flexible in all 20 models. In the most representative structure (model 1 – typically the selected conformer in the previous FIRST studies on NMR structures) both α -helices are rigid. Note there is a substantial difference in the size of these two rigid clusters over the ensemble. The blue cluster is the largest rigid cluster, however there is a switch across the models in which α -helix gets declared as blue or green. In some models, parts of, or even an entire α -helix (model 8) are flexible. This shift is particularly evident in the ends of α -helices, notably in the N-terminal end of α -helix 1, which has significantly weaker hydrogen bonding interactions than its C-terminal end.

It is known that small changes in conformation of atoms can lead to altered hydrogen bonding geometry (hydrogen bond energy values) (see [61]) and a consequent change in the total number of included hydrogen bond constraints. Hence, the variation in the size of the rigid clusters across the different NMR models with slight structural heterogeneity is not surprising. The number of hydrogen bonds with energies less than

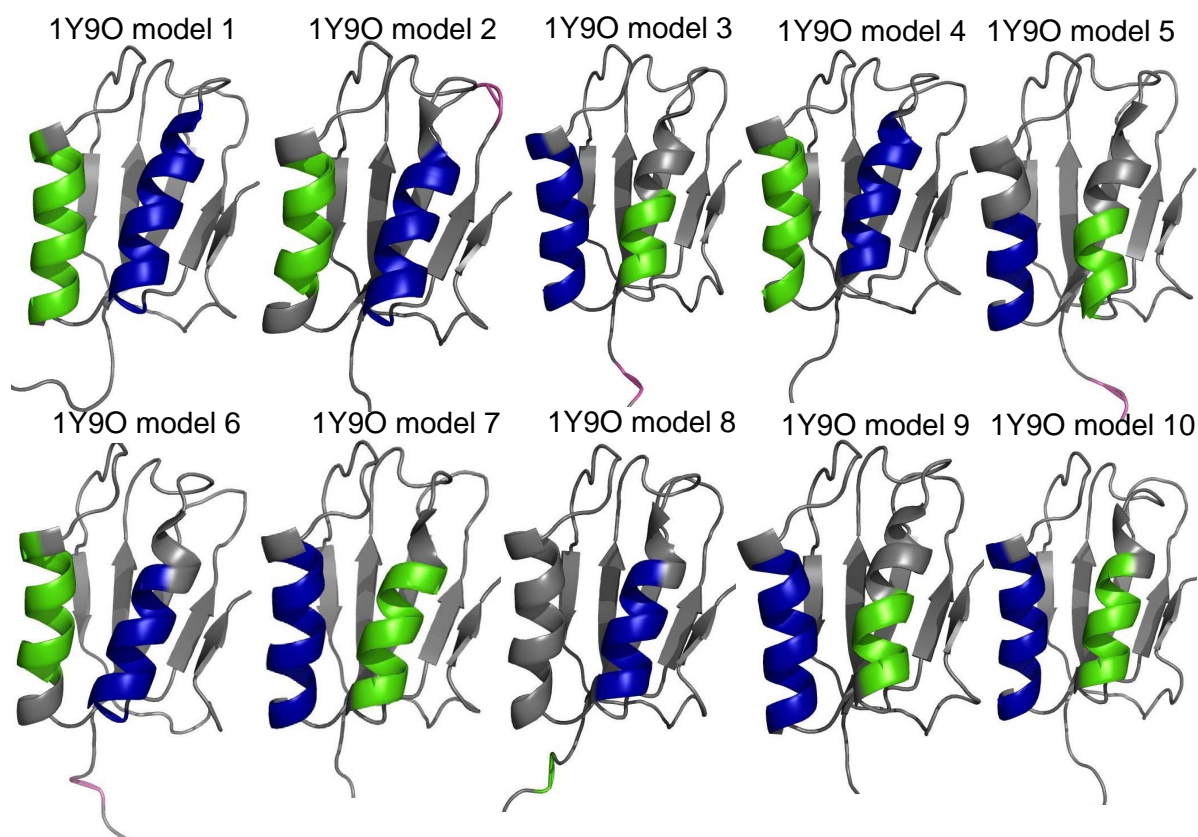


Figure 5. Rigid cluster decomposition using FIRST on NMR models of Sso AcP. The output of first 10 models from the ensemble is displayed. The blue rigid cluster is the largest rigid cluster, followed by the green rigid cluster. Note the variation in the size of the rigid clusters among the NMR models.

−1 kcal/mol among the 20 models of Sso AcP ranges from as few as 43 hydrogen bonds to as many as 54 hydrogen bonds. These differences will clearly have an effect on the total number of remaining DOF from model to model, and on the size of the rigid clusters. These observations are similar in flavour to the study by Wells et al. [61], where the authors found that FIRST analysis on structurally similar crystal structures with the same energy cutoff can produce different rigid cluster decompositions.

3.3. FIRST-ensemble results

The output of the FIRST-ensemble Algorithm 2.1 on Sso AcP is provided in figure 6. Over the ensemble, α -helix 2 retains most of its rigidity and becomes flexible only at its end points. On the other hand, roughly half of α -helix 1 is rigid, corresponding to its C-terminal half. In the flexible N-terminal half of α -helix 1 most of the hydrogen bonds are very weak (i.e. their average strengths do not pass the energy cutoff), or there is a lack of a sufficient number of persistent strong hydrogen bonds over the ensemble, which are modeled with less bars between hydrogen and acceptor atoms (Algorithm 2.1

step 3 (b)). As expected, the β -sheet remains flexible in the ensemble prediction.

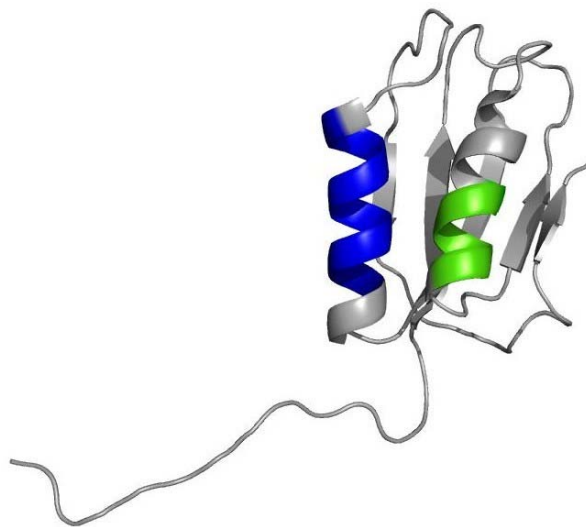


Figure 6. Rigid cluster decomposition from FIRST-ensemble, Algorithm 2.1. There are two main rigid clusters. Most of α -helix 2 is rigid (blue), with the exception of its end points. On the other hand, α -helix 1 is rigid on its C-terminal half (green), and flexible in the N-terminal half. The β -sheet is flexible.

Changes in the rigidity can be monitored by a gradual removal of hydrogen bonds one by one (i.e. by lowering of hydrogen bond energy cutoff) in the order of strength, keeping all covalent and hydrophobic interactions intact, and then redoing the rigidity analysis at each step identifying rigid and flexible regions. The change in rigidity can be visualized nicely using the hydrogen bond ‘dilution plot’ [34]. The dilution plot for FIRST-ensemble prediction on Sso AcP is shown in figure 7 (see [23, 24, 34, 61] for detailed explanation of dilution plots).

The fact that the β -sheet in Sso AcP is flexible and the α -helices are rigid is concordant with the study by Whiteley [63], which provides a precise rigidity-based characterization of flexibility and the minimum number of constraints needed for simple secondary structure motifs (i.e. rings, loops, α -helices, β -sheets and β -barrels) to become rigid in FIRST. With the exception of β -barrels, this study reminds us that an isolated β -sheet will only become rigid when there are a large number of strands or fewer strands but with longer lengths. On the other hand, an isolated α -helix (or part of) will attain its rigidity much more easily than a β -sheet [63]. Our rigidity analysis of Sso AcP is also consistent with previous FIRST analysis on other proteins. For instance, Wells et al. [61] have observed that as weak hydrogen bonds are broken (diluted), α -helices retain their rigidity much longer than β -sheets.

Even though the β -sheet of Sso AcP is flexible, it has a well-defined structure and a high number of persistent strong inter-strand hydrogen bonds over the entire ensemble. In figure 8 we have displayed the hydrogen bond constraints that are included in the FIRST-ensemble analysis. The strength of these persistent inter-strand hydrogen bonds in the β -sheet is also supported by the anti-parallel arrangement of the four β -strands

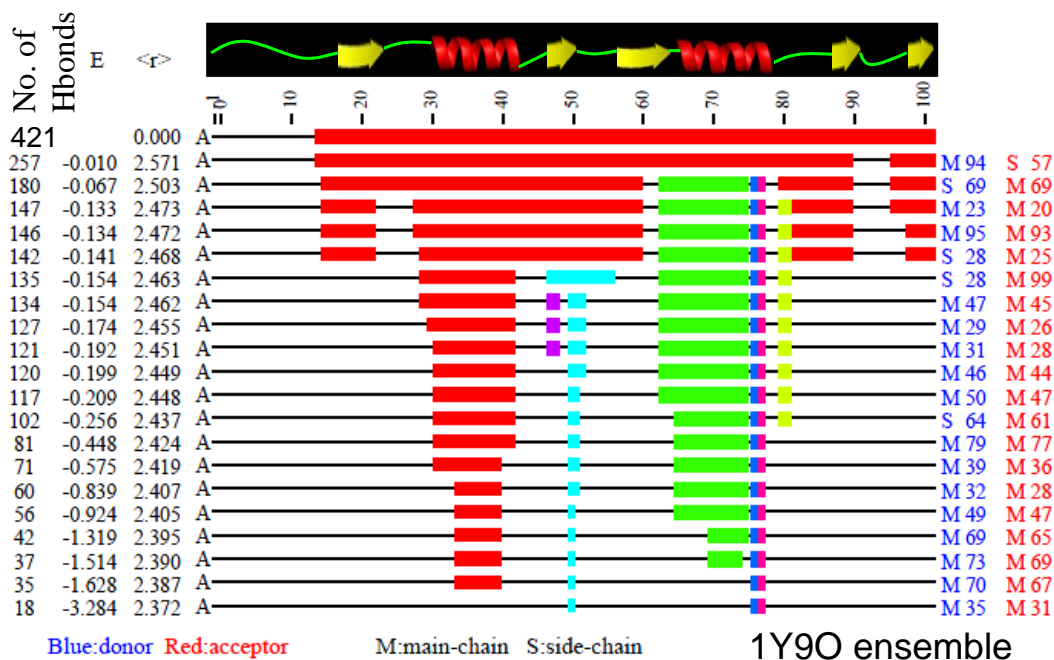


Figure 7. Dilution plot of FIRST-ensemble (Algorithm 2.1) on Sso AcP. Flexible regions are indicated with thin black lines, and rigid regions are indicated with blocks. The columns on the left-hand side are updated and display: the total number of remaining hydrogen bonds, the energy of the hydrogen bond that is currently broken in kcal/mol. The mean coordination number is also provided. The columns on the right represent the residue numbers of the donor and acceptor atoms of the broken hydrogen bond at each step. Initially, with inclusion of all potential hydrogen bonds from the entire ensemble, in the FIRST-ensemble prediction of Sso AcP the entire protein is rigid (top red block) with the exception of the long flexible tail at the N-terminus. Once most weak hydrogen bonds are broken (going down the dilution plot) several rigid clusters form, and it is evident from the dilution plot that β -sheets become flexible and essentially only two significant rigid clusters remain, corresponding to the two α -helices.

1 to 4, which gives rise to the preferred nearly planar hydrogen bond geometry between the NH and CO groups.

Normally β -sheets are rigidified with hydrophobic interactions and side chain hydrogen bonds. This occurs when β -sheets are well-packed against other β -sheets or α -helices, as is for instance the case in the amyloid-fibril formation via stacking of β -sheets, where there is both strong inter-strand and inter- β -sheet interactions [31]. The main reason the β -sheet of Sso AcP is flexible is due to the lack of these additional constraints within the strands or between the β -sheet and α -helices. Most of these hydrogen bonds are very weak with energies close to 0 kcal/mol. It seems that the importance of the side chain hydrogen bonding interactions and hydrophobic contacts to rigidity of β -sheets has not been explicitly commented or investigated in the FIRST literature.

The clear advantage of the FIRST-ensemble prediction over the traditional

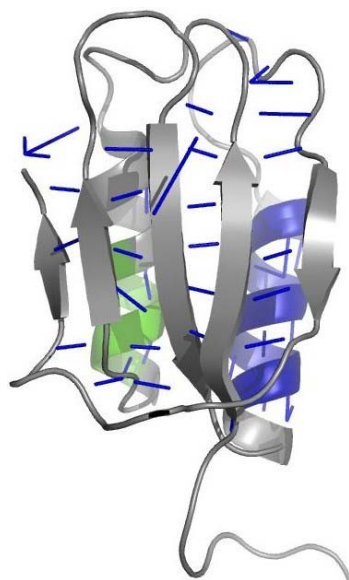


Figure 8. Output of FIRST-ensemble, same as in figure 6 with a different orientation. There are a significant number of strong inter-strand hydrogen bonds (indicated with blue lines) that are present in the flexible β -sheet.

FIRST runs performed on NMR files using a single snapshot is that FIRST-ensemble incorporates the structural information from the entire NMR ensemble. By averaging the hydrogen bonding strengths and incorporating persistence of hydrogen bonds from all structures, with FIRST-ensemble prediction we can capture the variations in the rigid clusters between individual models of Sso AcP; (Note that averaging hydrophobic interactions is not essential for ensemble rigidity predictions - see Supplementary information). Furthermore, in contrast to the previous FIRST study [21], where the authors performed rigidity analysis on all individual MD generated snapshots, and then averaged rigidity results (i.e. flexibility index), our FIRST-ensemble prediction is attained using only a single adapted FIRST run. This way we can continue to utilize and take advantage of the fast computational speed of FIRST, and at the same time incorporate the structural information from entire ensemble.

As was discussed earlier, rigidity and flexibility prediction on its own does not lead to a conclusive measure of HDX as we also need solvent accessibility. However, it is already evident that the FIRST-ensemble predictions are much better matched with the experimental HDX data on Sso AcP than the traditional FIRST run using a single NMR snapshot. In the FIRST prediction on the most representative model, both α -helices are entirely rigid, while in the FIRST-ensemble prediction, α -helix 2 is mostly rigid with its ends becoming flexible, and only half of α -helix 1 comes up as rigid. This is in agreement with the experimental HDX data, where roughly half of α -helix 1 and most of α -helix 2 (except its ends) are protected from HDX (Figure 4). It is certainly not uncommon for parts of α -helices to be unstructured and flexible, but considering the hypothermophile nature of this protein, it is remarkable that FIRST-ensemble is able

to capture sub-structural flexibility of α -helix 1. Clearly, in using only one structure out of the ensemble as an input into FIRST, important structural variations across the ensemble are lost, particularly the conformational variations in the N-terminal half of α -helix 1. On both α -helices, the FIRST-ensemble predicted rigid regions give a very good indication of the regions that will be protected from HDX. Since the rest of the protein is flexible, we cannot yet draw any definite comparisons or conclusions with respect to the HDX data (see solvent accessibility of Sso AcP).

3.4. Solvent Accessibility ensemble data

The plot of solvent accessibility (RSA) for the backbone amide Nitrogens of Sso AcP, averaged over the ensemble, is given in figure 9. In figure 10 we have coloured the structure with the solvent accessibility colouring scheme as described in section 2.4. The first striking observation is that the three β -strands (strands 1, 2 and 3) are completely buried. In fact, almost every residue in these three strands has 0% average solvent accessibility. Having no backbone amide (NH) accessibility over the ensemble suggests that these strands should be well protected from undergoing HDX. Indeed, the experimental HDX data confirms that the three central β -strands (three blue strands in figure 4) are the slowest exchangers (best protected from undergoing HD-exchange). The two side strands are more solvent accessible. β -strand 4, located behind α -helix 2 has both buried and almost completely exposed amides. At the C-terminus of strand 4, the backbone amide Nitrogen of residue Phe87 is almost completely exposed (47 % accessibility) as it is directed towards the solvent. It is bound by two completely buried (0 % accessible) Ser86 and Ser88, whose amide protons are pointing towards the Sso AcP structural core. This is also in good correspondence with the experimental HDX, where a ‘Very Fast’ Phe87 exchanger is bounded by two ‘Very Slow’ serine exchangers (Figure 4). β -strand 5, the short strand located at the opposite edge of the β -sheet appears to be overall more solvent accessible. This again is in reasonable agreement with the experimental HDX.

We had indicated earlier that we will not use solvent accessibility data on α -helices, as it is not a reliable indicator of HDX due to the amphipathic nature of α -helices. As anticipated, we found that the α -helices of Sso AcP have mixed solvent accessibility. This becomes visually apparent with the side view orientation of the protein (Figure 10 (b)). Here we observe that the two sides of α -helices that are facing one another or the sides facing the β -sheet are mostly buried, while the opposite sides are more solvent exposed. In the N-terminal half of α -helix 1, several residues have very low accessibility (Arg30 and Val33 are almost completely buried, Ly31 is only somewhat exposed), yet we have already seen that this flexible half of α -helix 1 is very unstructured, and from experimental HDX evidence it does not represent a slow exchanging part of the protein. Similarly, solvent accessibility data on α -helix 2 would not be a good predictor of HDX, and is not well agreed with the experimental HDX profile.

In addition to the amphipathic nature of α -helices, we can envision other reasons

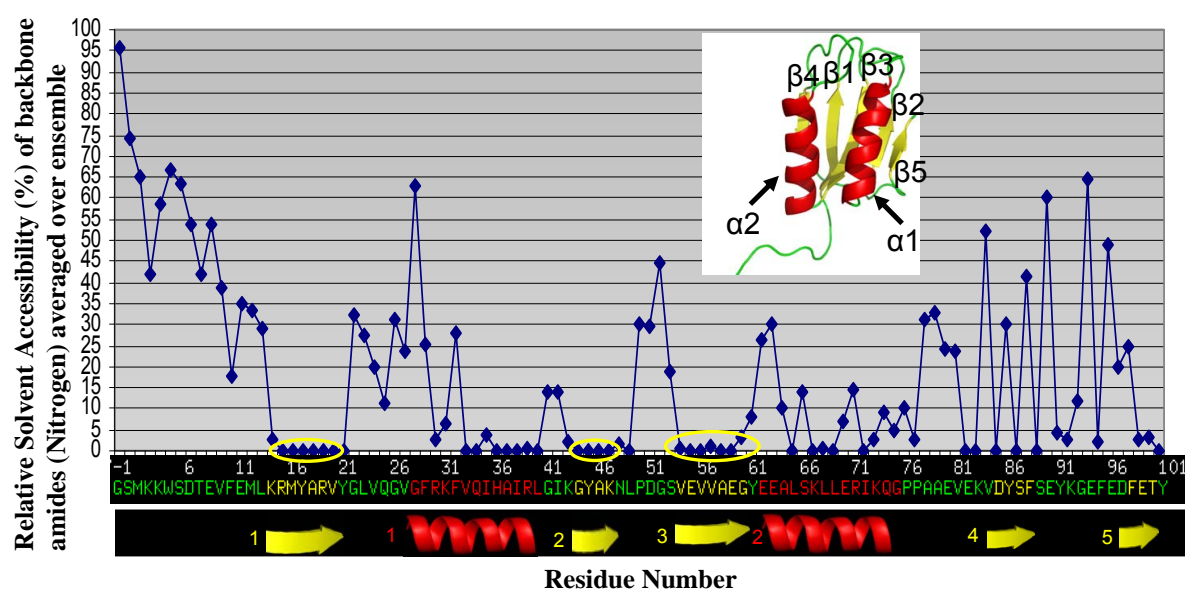


Figure 9. Solvent accessibility (RSA) of Sso AcP of backbone amide (NH) averaged over the ensemble; obtained from WHATIF [58]. Note the three central β -strands (strand 1, 2, and 3, circled in yellow) are almost completely buried.

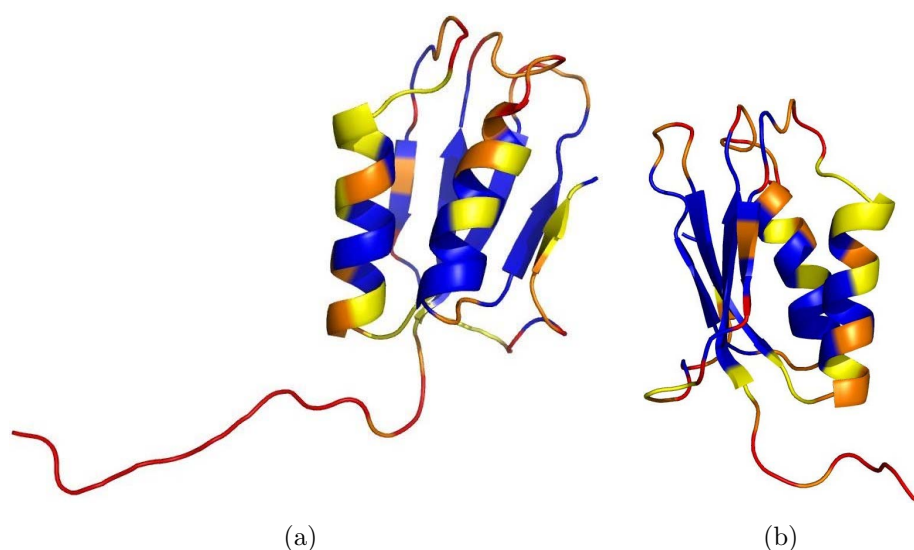


Figure 10. Solvent accessibility (RSA) of Sso AcP of backbone amide (NH) averaged over the ensemble. The blue regions are almost completely buried (solvent inaccessible) (RSA \leq 4%), followed by yellow regions - somewhat exposed, orange - mostly exposed, and red - almost completely exposed (a). Same display with different orientation (b) which indicates the mixed accessibility of α -helices, with the more buried side pointing towards the interior of the protein.

why solvent accessibility on α -helices is not a sufficient measure to probe HDX. Unlike β -sheets, which can be predicted as flexible by FIRST and yet have a well-defined structure with strong inter-strand hydrogen bonding network, substructural flexibility

in an α -helical structure is a direct consequence of weak α -helical hydrogen bonding interactions. In the flexible regions of an α -helix, the backbone amides are not involved in hydrogen bonding for the maintenance of secondary structure. So, even if part of the flexible α -helix is computationally predicted to be buried on a snapshot(s), this region of a α -helix can still potentially undergo backbone motions and turn a previously buried backbone amide proton into a solvent exposed amide proton. In such a case HDX could still occur.

In summary, solvent accessibility on Sso AcP gives a good estimate of HDX on the β -sheet, and a poorer prediction on α -helices as was expected. The remaining flexible regions (loops and the long flexible tail) are mostly solvent accessible, and still correspond well with the experimentally determined fast HD-exchangers. It is well known that flexible and highly mobile regions in the protein are likely to be solvent accessible [67]. As we are calculating the average solvent accessibility over the ensemble, any highly flexible region that retains its solvent accessibility over the entire ensemble has a higher likelihood to remain solvent accessible.

3.5. Combined rigidity and solvent accessibility predictions of HDX on Sso AcP

Rigidity (FIRST-ensemble) predictions and solvent accessibility measures are valuable tools to computationally probe HDX. We have seen that on their own, rigidity or solvent accessibility, would lead to an inefficient overall predictor. By incorporating both analysis, an improved prediction of HDX can be achieved.

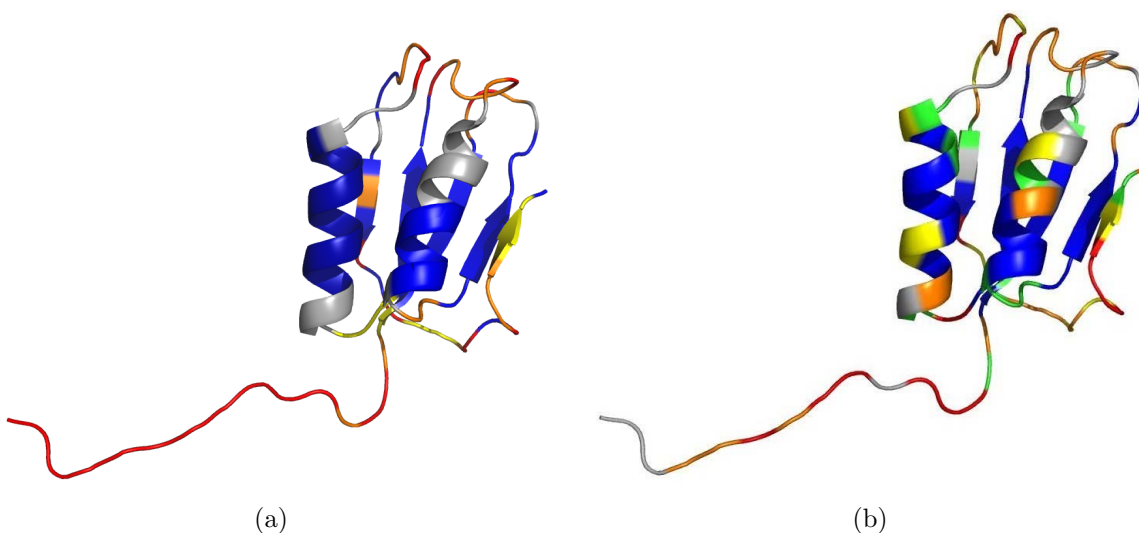


Figure 11. Combined rigidity (FIRST-ensemble) and solvent accessibility on Sso AcP, see Algorithm 2.2 (a), and experimentally derived HDX profile of Sso AcP (b). The blue regions (computationally predicted to not undergo HDX) in (a) (obtained by combining the rigid clusters and buried residues) match exceptionally well with the experimentally determined slow exchangers. The remaining regions are also in a good agreement.

The combined FIRST-ensemble rigid clusters and solvent accessibility on Sso AcP is shown in figure 11 (a) (see Algorithm 2.2). We recall that the blue region in the α -helices corresponds to the two rigid clusters found by FIRST-ensemble algorithm (Figure 6). The remaining blue regions (notably the three central β -strands) and some residues in β -strand 1 represent the ‘solvent inaccessible’ regions. These (combined) blue regions are the predicted regions in the protein that will be protected from undergoing HDX (i.e. slowest exchangers). Comparing this computational prediction with the experimentally obtained HDX profile of Sso AcP, the predicted HDX protected regions are in very good agreement with the experimentally determined very slow exchangers. For richer visual display of these results, in figure 12 we have presented both computational predictions and experimentally determined slow exchangers on a 1-dimensional (backbone) representation of the protein.

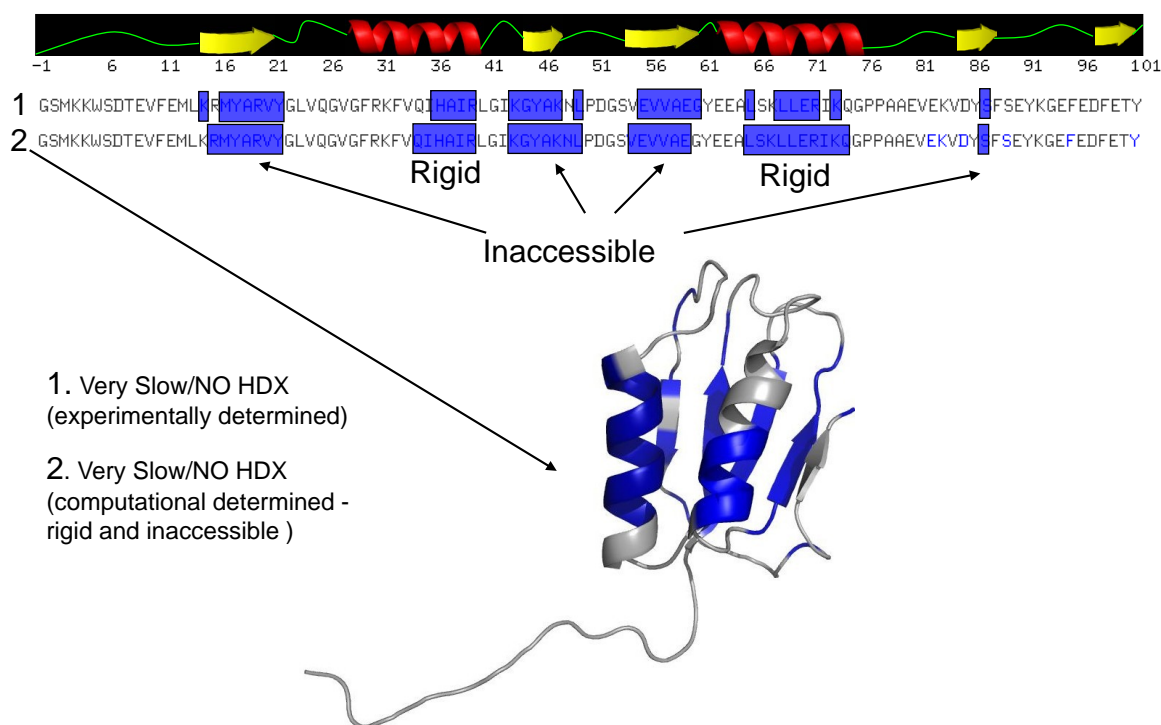


Figure 12. Comparison of the computationally predicted secondary structure residues that are least likely to undergo exchange with the experimentally determined slowest exchangers is illustrated on the backbone protein chain. In line 1 the blue regions represent the experimentally determined very slow exchangers (most protected residues). Line 2 depicts the computationally predicted slowest exchangers composed of rigid and almost completely buried residue. The computational predictions are remarkably well matched with experimentally determined very slow exchangers on all the major secondary structure regions.

In summary, our computational approach gives a very good prediction of the regions that remain most protected from exchange which is supported by experimental HDX data. We have obtained a good prediction on the loops and the N-terminus tail, but

as expected these regions are highly flexible and unstructured (a few stable hydrogen bonds), and are harder to probe than the secondary structures. Our findings on Sso AcP support our hypothesis that combined rigidity-solvent accessibility predictions can be used to probe HDX.

4. Conclusion and Outlook

The aim of this study was twofold: to introduce a novel technique for computing rigidity of ensembles using the FIRST method and to show that combining rigidity and solvent accessibility can lead to good fast computational predictions of HDX, as it was applied on a hyperthermophile protein Sso AcP.

We found that there is a significant variation in the rigid cluster decompositions across individual NMR models. FIRST-ensemble prediction incorporates the structural information and variations from all the models and we have shown that the ensemble rigid cluster decomposition is best matched with experimental HDX on Sso AcP. From our findings on Sso AcP, and general analysis on FIRST in [61], we suggest that the FIRST rigidity analysis on NMR ensembles or other sources of ensemble data (i.e. MD snapshots) should be based on the FIRST-ensemble predictions to make them more robust. As part of future work, for comparison and further validation, it would be valuable to apply our FIRST-ensemble algorithm on a larger class of NMR proteins, where it would be desired to have comparable experimental data, such as the high coverage native state HDX profile on Sso AcP we obtained in this study. The methods and techniques developed in this paper should further enhance the capability of FIRST and offer new tools and research avenues in predicting rigidity of ensembles. In other current work [52], using rigidity adapted coarse graining MD simulations, initial results suggest that FIRST-ensemble analysis on NMR file of hemagglutinin fusion-peptide gives an improved rigidity prediction compared to the single snapshot FIRST analysis.

Both rigidity and solvent accessibility are important tools in probing HDX, but best prediction is achieved when these measures are combined. We have shown that our combined ensemble rigidity/accessibility algorithmic predictions on Sso AcP is well matched with the experimental HDX profile of Sso AcP. In the last 10 years there has been a rapidly growing interest in applying rigidity based techniques to study both flexibility and motions of proteins, RNA and DNA. To the best of our knowledge, this is the first study that incorporates rigidity and accessibility as a computational method for predicting HDX. The clear advantage of these techniques is that they offer very fast computational technique in probing an expensive and laborious experimental method.

Acknowledgements.

We thank Walter Whiteley for many extended discussions on applications of rigidity theory to protein flexibility and valuable feedback on this paper. We are also grateful to Fabricio Chiti for supplying the Sso AcP expression vector.

References

- [1] Aszodi A and Taylor WR 2005 Protein Geometry, Classification, Topology and Symmetry, A computational Analysis of Structure, Series in Biophysics, Taylor and Francis, New York.
- [2] Bai Y and Sosnick TR, Mayne L and Englander SW 1995 Protein folding intermediates: native-state hydrogen exchange, *Science*, Vol. 269 no. 5221 pp. 192-197.
- [3] Bain AD and Burton IW 1996 *Concepts in Magnetic Resonance* 8, 191-204.
- [4] Bemporad F, Gsponer J, Hopearuoho HI, Plakoutsi G, Stati G, Stefani M, Taddei N, Vendruscolo M and Chiti F 2008 Biological function in a non-native partially folded state of a protein, *The EMBO Journal*, 27, 15251535.
- [5] The Brookhaven Protein Data Bank (PDB), <http://www.pdb.bnl.gov>.
- [6] Case DA 1999 Molecular dynamics and normal mode analysis of biomolecular rigidity. In: Thorpe MF, Duxbury PM, eds. *Rigidity Theory and Applications*. New York: Kluwer Academic/Plenum Publishers; pp 329344.
- [7] Chothia C 1976, The nature of the accessible and buried surfaces in proteins, *J. Mol. Biol.* 105, 142.
- [8] Corazza A, Rosano C, Pagano K, Alverdi V, Esposito G, Capanni C, Bemporad F, Plakoutsi G, Stefani M, Chiti F, Zuccotti S, Bolognesi M and Viglino P 2006 Structure, Conformational Stability, and Enzymatic Properties of Acylphosphatase From the Hyperthermophile *Sulfolobus solfataricus*, *Proteins*, 62, 64-79.
- [9] Daniel RM, Dunn RV, Finney JL and Smith JC 2003 The Role of Dynamics in Enzyme Activity, *Annu. Rev. Biophys. Biomol. Struct.*, 32:6992.
- [10] Delaglio F, Grzesiek S, Vuister GW, Zhu G, Pfeifer J and Bax AJ 1995 *Biomol. NMR* 6, 277-293.
- [11] Dill KA and Chan HS 1997 *Nature Structural Biology*, 4, 10-19.
- [12] Dovidchenko NV and Galzitskaya OV 2008 Prediction of Residue Status to Be Protected or Not Protected From Hydrogen Exchange Using Amino Acid Sequence Only, *The Open Biochemistry Journal*, 2, 77-80.
- [13] Eisenmesser E, Millet O, Labeikovsky W, Korzhnev DM, Wolf-Watz M, Bosco DA, Skalicky JJ, Kay LE and Kern D 2005 Intrinsic dynamics of an enzyme underlies catalysis, *Nature*, 438, 117-121.
- [14] Englander SW and Kallenbach NR 1983 Hydrogen exchange and structural dynamics of proteins and nucleic acids, *Q. Rev. Biophys.* 16 (4): 521655.
- [15] Englander SW, Mayne L, Bai Y, Sosnick TR 1997 Hydrogen exchange: the modern legacy of Linderström-Lang, *Protein Sci.* 6, 1101-1109.
- [16] Flexweb Server (FIRST), <http://flexweb.asu.edu>.
- [17] Frauenfelder H, McMahon BH, Austin RH, Chu K and Groves JT 2001 The role of structure, energy landscape, dynamics, and allostery in the enzymatic function of myoglobin, *Proc Natl Acad Sci*;98:23702374.
- [18] Fulle S and Gohlke H 2008 Analysing the flexibility of RNA structures by constraint counting, *Biophys J* 94:4202-4219.
- [19] Getz M, Sun X, Casiano-Negróni A, Zhang Q, and Al-Hashimi HM 2007 NMR studies of RNA dynamics and structural plasticity using NMR residual dipolar couplings, *Biopolymers*, 86:384-402.
- [20] Goddard TD and Kneller DG 2002 SPARKY 3, University of California, San Francisco.
- [21] Gohlke H, Kuhn LA, Case DA 2004 Change in protein flexibility upon complex formation: Analysis of ras-raf using molecular dynamics and a molecular framework approach, *Proteins*, 56 (2), 322337.
- [22] Goodey NM and Benkovic SJ 2008 Allosteric regulation and catalysis emerge via a common route, *Nature Chemical Biology*, volume 4 number 8.
- [23] Hespenheide BM, Kuhn LA, Rader AJ and Thorpe MF 2002 Identifying protein folding cores from the evolution of flexible regions during unfolding, *J Mol Graph Model*, 21:195-207.

- [24] Hespenheide BM, Kuhn LA, Rader AJ and Thorpe MF 2002 Protein unfolding: rigidity lost, *Proc Natl Acad Sci U S A*, 99:3540-5.
- [25] Hespenheide BM, Jacobs DJ and Thorpe 2004 Structural rigidity in the capsid assembly of cowpea chlorotic mottle virus, *J. Phys.: Condens. Matter* 16 S5055-64.
- [26] Hubbard SJ and Thornton JM 1993 NACCESS, Department of Biochemistry and Molecular Biology, University College, London.
- [27] Hvidt A and Nielsen SO 1996 Hydrogen Exchange in Proteins, *Advances in Protein Chemistry*, *Advances in Protein Chemistry*, 21, 287-386.
- [28] Hwang TL, Shaka AJ 1995 *J. Magn. Reson. A*, 112, 275-279.
- [29] Hwang TL, van Zijl PCM, Mori S 1998 *J. Biomol. NMR*, 11, 221-226.
- [30] Krishna MMG, Maity H, Rumbley JN, Lin Y and Englander SW 2006 *J. Mol. Biol.*, 359, 1410-1419.
- [31] Knowles T and Buehler MJ 2011 Nanotechnology of functional and pathological amyloid materials, *Nature Nanotechnology*, Vol 6(7), 469-479.
- [32] Kondrashov DA, Zhang W, Aranda R, Stec B and Phillips GN Jr 2008 Sampling of the native conformational ensemble of myoglobin via structures in different crystalline environments, *Proteins: Structure, Function, and Bioinformatics*, 70: 353-362.
- [33] Krebs WG and Gerstein M 2000 The morph server: a standardized system for analyzing and visualizing macromolecular motions in a database framework. *Nucleic Acids Research*; 28:1665-1675.
- [34] Kuhn LA, Rader DJ and Thorpe MF 2001 Protein flexibility predictions using graph theory, *Proteins*, 44:150-65.
- [35] ProFlex, www.bch.msu.edu/~kuhn/software/proflex/index.html
- [36] Labeikovsky W, Eisenmesser EZ, Bosco DA and Kern D 2007 *J. Mol. Biol.*, 367, 1370-1381.
- [37] Lee A and Streinu I 2005 Pebble Game Algorithms and (k, l)-sparse graphs, 2005 European Conference on Combinatorics, Graph Theory and Applications (EuroComb 05), DMTCS Proceedings: 181186.
- [38] Levin EJ, Kondrashov DA, Wesenberg GE and Phillips GN Jr 2007 Ensemble refinement of protein crystal structures validation and application, *Structure*, 15(9): 10401052.
- [39] Lins L, Thomas A and Bresseur R 2003 Analysis of accessible surface of residues in proteins, *Protein Science*, 12:14061417.
- [40] Liu T, Pantazatos D, Li S, Hamuro Y, Hilser VJ and Woods VL Jr 2011 Quantitative Assessment of Protein Structural Models by Comparison of H/D Exchange MS Data with Exchange Behavior Accurately Predicted by DXCOREX, *J. Am. Soc. Mass Spectrom*, 23(1):43-56.
- [41] Ma B, Kumar S, Tsau C-J and Nussinov R 1999 Folding funnels and binding mechanisms, *Protein Engineering*, vol. 12, no. 9, pp. 713-720.
- [42] Mamonova T, Hespenheide B, Straub R, Thorpe MF and Kurnikova M 2005 Protein flexibility using constraints from molecular dynamics simulations, *Phys. Biol.* 2, S137S147.
- [43] Ming D, Kong Y, We Y and Ma J 2003 Substructure synthesis method for simulating large molecular complexes *Proc. Natl Acad. Sci. USA* 100 1049.
- [44] Momen-Roknabadi A, Sadeghi M, Pezeshk H and Marashi SA 2008 Impact of residue accessible surface area on the prediction of protein secondary structures, *BMC Bioinformatics* 9:357.
- [45] Mori S, Abeygunawardana C, Johnson MO and Vanzijl PCM 1995 *J. Magn. Reson. B*, 108, 94-98.
- [46] Perez A, Noy A, Lankas F, Luque FJ and Orozco M 2004 The relative flexibility of B-DNA and A-RNA duplexes: Database analysis, *Nucleic Acids Res*, 32:6144-6151.
- [47] Phillips GN 2009 Describing protein conformational ensembles: beyond static snapshots, *F1000 Biol Reports*, 1:38.
- [48] PYMOL, <http://pymol.sourceforge.net/>.
- [49] Radestock S and Gohlke H 2008 Exploiting the Link between Protein Rigidity and Thermostability for Data-Driven Protein Engineering, *Eng. Life Sci.* 8, No. 5, 507522.
- [50] Rost B and Sander C 1994 Conservation and prediction of solvent accessibility in protein families. *Proteins*, 20:216226.

- [51] Sadqi M, Casares S, Abril MA, Lopez-Mayorga O, Conejero-Lara F and Freire E 1999 The native state conformational ensemble of the SH3 domain from alpha-spectrin., *Biochemistry*, 38(28):8899-906.
- [52] Sammadi M, Vaidya N, Sljoka A and Huaxiong H 2013 Coarse graining molecular dynamics with rigidity of hemagglutinin fusion peptides, preprint.
- [53] Schulze B, Sljoka A and Whiteley W 2013 How does symmetry impact the flexibility of proteins?, to appear in *Philosophical Transactions, Royal Society*.
- [54] Shatsky M, Nussinov R and Wolfson HJ 2002 Flexible protein alignment and hinge detection. *Proteins*, 48:242256.
- [55] Sheu SY, Schlag EW, Selzle HL and Yang DY 2009 Hydrogen Bonds in Membrane Proteins, *J. Phys. Chem.*.
- [56] Sljoka A 2012 *Algorithms in rigidity theory with applications to protein flexibility and mechanical linkages*, PhD Thesis, York University, <http://www.math.yorku.ca/~adnanslj/adnanthesis.pdf>.
- [57] Thorpe MF, Jacobs DJ, Chubynsky NV and Rader AJ 1999 Generic rigidity of network glasses. In: Thorpe MF, Duxbury PM, eds. *Rigidity theory and applications*. New York: Kluwer Academic/Plenum Publishers, pp 239277.
- [58] Vriend G 1990 WHAT IF, A molecular modelling and drug design program. *J. Mol. Graphics*, 8, 5256 <http://swift.cmbi.ru.nl/whatif>.
- [59] Vranken W 2007 A global analysis of NMR distance constraints from the PDB, *J Biomol NMR.*, 39(4): 303314.
- [60] Wells SA, Menor S, Hesperheide BM and Thorpe MF 2005 Constrained geometric simulation of diffusive motion in proteins, *Phys. Biol.*, 2 S12736.
- [61] Wells SA, Jimenez-Roldan JE and Romer RA 2009 Comparative analysis of rigidity across protein families, *Phys. Biol.* 6, 046005.
- [62] Whiteley W 1999 Rigidity of molecular structures: generic and geometric analysis, *Rigidity theory and applications*, M.F. Thorpe and P.M. Duxbury, Editors, Academic/Kluwer. p. 21-46.
- [63] Whiteley W 2005 Counting out to the flexibility of molecules, *Phys. Biol.* 2, S116-S126.
- [64] Wolf-Watz M, Vu T, Henzler-Wildman K, Hadjipavlou G, Eisenmesser EZ and Kern D 2004 *Nat. Struct. Mol. Biol.*, 11, 945-949.
- [65] Woodward C, Simon I and Tuchsien I 1982 Hydrogen-exchange and the Dynamic Structure of Proteins, *Mol. Cell. Chem.*, 48(3): 135-160.
- [66] Zhang YZ 2001 *Sphere: Protein and peptide structure and interactions studied by hydrogen exchange and NMR*, PhD Thesis, University of Pennsylvania.
- [67] Zhang H, Zhang T, Chen K, Shen S, Ruan J and Kurgan L 2009 On the relation between residue flexibility and local solvent accessibility in proteins, *Proteins*, 76:617636.